Plant Physiol. (1983) 71, 719–730
0032-0889/83/71/0719/12/$00.50/0

Regulation of Cell Shape in *Euglena gracilis*

I. INVOLVEMENT OF THE BIOLOGICAL CLOCK, RESPIRATION, PHOTOSYNTHESIS, AND CYTOSKELETON

Received for publication June 29, 1982 and in revised form November 17, 1982

THOMAS A. LONERGAN
Department of Biological Sciences, University of New Orleans, New Orleans, Louisiana 70148

ABSTRACT

The alga *Euglena gracilis* Z. changes its shape two times per day when grown under the synchronizing effect of a daily light-dark cycle. At the beginning of the light period when photosynthetic capacity is low, the population of cells is largely spherical in shape. The mean cell length of the population increases to a maximum in the middle of the light period when photosynthetic capacity is greatest, and then decreases for the remainder of the 24-hour period. The population becomes spherical by the end of the 24-hour period when the cycle reinitiates. These changes are also observed under constant dim light conditions (up to 72 hours) and are therefore controlled by the biological clock and represent a circadian rhythm in cell shape. In constant dim light, the cell division rhythm is either arrested or slowed considerably, while the cell shape rhythm continues.

The involvement of respiratory and photosynthetic pathways in the cell shape changes was investigated with energy pathway inhibitors. Antimycin A and NaN_3 both inhibited the round to long and long to round shape changes, indicating that the respiratory pathways are involved. DCMU and atrazine inhibited the round to long shape change but did not affect the long to round transition, indicating that light-induced electron flow is necessary only for the round to long shape change.

The influence of the cell shape changes on the photosynthetic reactions was investigated by altering cell shape with the cytoskeletal inhibitors cytochalasin and colchicine. Both inhibitors blocked the round to long and long to round shape changes. Cytochalasin B was found to have minimal cytotoxic effects on the photosynthetic reactions, but colchicine significantly inhibited light-induced electron flow and the *in vivo* expression of the photosynthetic rhythm.

The cell shape characteristic of an algal species may be determined by the presence of a cell wall (16, 18), cytoskeletal components (4, 10, 20, 27, 28), a pellicle beneath the plasma membrane (18, 20), or osmotic properties of the cell (22).

Euglena gracilis is a highly studied flagellated alga that displays numerous shape changes. The shape of the *Euglena* cell may change depending on whether the cells are grown in the light or dark (6, 20), or exhibit the many changes characteristic of the twisting movements related to swimming called metaboly (euglenoid movement) (2). The biological clock has also been implicated in the regulation of cell shape. A daily rhythm in the average cell volume of a synchronous *Euglena* population has recently been reported (17) and a possible daily rhythm in cell shape was implied by Brinkmann (6).

This study reports that the cell length of *Euglena* changes in a predictable rhythmic manner each day, and that the changes are under the control of the biological clock. The biological clock control of cell shape offers a unique opportunity to study naturally occurring shape changes that repetitively occur within a predictable time scale. This investigation reports on the involvement of the respiratory and photosynthetic pathways in the daily shape changes, and a preliminary characterization using cytoskeletal inhibitors to determine whether the expression of the rhythm in photosynthetic capacity is dependent upon the rhythm in cell shape.

MATERIALS AND METHODS

Cell Cultures. *Euglena gracilis* Z. was procured from the American Type Culture Collection and was maintained as previously reported (25, 26). Aliquots from liquid stocks were added to 250-ml flasks containing 200 ml liquid medium. Cultures were exposed to a 10-h light, 14-h dark cycle with a light intensity of 300 μE m^{-2} s^{-1}. Cultures were magnetically stirred and aerated with filter-sterilized room air at a rate of 0.5 L min^{-1}. When required by experimental design, cultures were exposed to constant dim light of 3.5 μE m^{-2} s^{-1} intensity.

Measurement of Cell Length. Aliquots of the cultures were removed by syringe and centrifuged in a clinical centrifuge for 30 s. The cell pellet was resuspended in a few drops of 10% formalin to fix the cells for photography. Cells were photographed at × 100 magnification using a Leitz Ortholux microscope equipped with a 35-mm camera using Kodak Pan Plus X film. The greater dimension of each cell was measured directly from the enlarged photographs using a draftsman ruler with each inch divided into 100ths. The photographs were enlarged so that 0.01 inch represented 1 μm on the photograph. A × 7 magnifying lens was used to increase the accuracy of readings when using the ruler. Approximately 200 to 250 measurements were obtained for each time point of each experiment. All cells in the photographs were measured to avoid bias, and photographs were measured using a blind coding technique so that there was no knowledge of which data points the photographs represented.

Volume Measurements. The volume of cells was estimated from measurements recorded from the photographs. Volume calculations were only recorded for the two shape extremes for which equations can be easily applied. Spherical cells in the size class 15 to 25 μm diameter were measured, and the formula $V = \frac{4}{3}\pi r^3$ was used to determine volume. The diameter of the cells was measured and the radius was determined as $D/2$. Cells in the 35 to 44-μm size class whose shape approximated a prolate spheroid (cigar-shaped with rounded ends) were measured and the formula $V = \frac{4}{3}\pi ab^2$ was used to determine the volume. The value a represents the semimajor axis of the cell (length of cell/2) while b represents the semiminor axis (width of cell/2). Cells of other shapes were not included in these calculations.

Respiration and Photosynthesis Measurements. Respiration and photosynthesis were measured using the O_2 electrode system previously reported (25, 26).

Light Intensity Plots. Light intensity was altered with a set of calibrated Balzer neutral density filters and measured with a Li-Cor quantum meter. New cell aliquots were used for the O_2 measurements at each light intensity. A cell density of approximately 1.5×10^5 cells/ml was used. The data were converted from the hyperbolic form to a linear form by plotting the data as light intensity/photosynthetic rate *versus* light intensity (26). The slope of the line is inversely proportional to the maximal photosynthetic rate. The slope and y intercept were calculated by linear regression.

Chloroplast Isolation. Chloroplasts were isolated as previously described (26). Cells were resuspended in an isolation medium consisting of 0.4 M sorbitol, 0.1 M Tricine (pH 7.8) at 20°C. Cells were broken by two 30-s sonication pulses (Braunsonic 1510 sonicator, B. Braun Co.) at 75-w output using the microprobe. The sonication was gentle and resulted in a 50% cell breakage. Chl was determined by the method of Arnon (1).

Whole Chain Electron Flow. The rate of light-induced electron flow through the entire electron transport chain was measured by determining O_2 consumption of chloroplasts in the presence of MV.[1] The reaction components have been previously described (26).

Use of Inhibitors. Water-soluble inhibitors were dissolved in the growth medium of Cramer and Myers (12) before addition to the culture. The choice of solvents for water-insoluble reagents (DCMU, DBMIB, antimycin A, gramicidin, and cytochalasin, Sigma) was found to affect the cell shape. Ethanol, at concentrations as low as 0.1% (v/v), caused all cells to become spherical within 30 min of exposure. This phenomenon was observed at all times of day but no investigations into this phenomenon were made. DMSO was found to be a more suitable solvent and concentrations as high as 1% had no effect on cell shape. Control cultures were divided into two equal halves in separate flasks before inhibitor addition. Inhibitors were added to one of the cultures at CT 24 (representing presumptive dawn, day 2 of the experiment), while no inhibitor was added to the other until CT 29 (5 h later). Cultures with inhibitors were aerated and stirred as previously indicated. A cell density of 1.5×10^5 cells/ml was used for all experiments.

Lumicolchicine, the UV-irradiated derivative of colchicine, was made by irradiating a 25 mM stock solution of colchicine (in Cramer and Myers growth medium) for 4 h. A Blak-Ray long wavelength UV lamp (Model xx15, Ultra-Violet Products, Inc.) was placed 5 cm above a 10-ml solution in an uncovered Petri plate placed on aluminum foil. Absorption spectroscopy of the lumicolchicine revealed absorption peaks at 138, 152, 160, 210, and 265 nm while colchicine had peaks at 155, 206, 245, and 350 nm, both in good agreement with spectra reported previously (32).

Statistical Analysis. The percentages of the population residing in three size classes, 15 to 24, 25 to 34, and 35 to 44 μm in length, were determined for each population. To determine whether the percentage of cells in one or more size classes was different from another population, tests were performed to determine the significance of differences between two percentages, control *versus* experimental. The test statistic is

$$t_s = \frac{\text{arcsine } \sqrt{P_1} - \text{arcsine } \sqrt{P_2}}{\sqrt{820.8(1/n_1) + (1/n_2)}}$$

where P_1 and P_2 are the proportions in the size class in the two samples, n_1 and n_2 are respective sample sizes, and 820.8 is a constant representing the parametric variance of a distribution of arcsine transformations of percentages (34). The arcsine is the angle, in degrees, whose sine corresponds to the value given and was determined from published tables (31). The t_s values were compared to critical values of Student's t distribution using a two-tailed distribution and 95% confidence limits.

[1] Abbreviations: MV, methyl viologen; DBMIB, 2,5-dibrom-3-methyl-6-isopropyl-*p*-benzoquinone; DMSO, dimethyl sulfoxide; CT, circadian time (time in hours beginning with the first transition from dark to constant dim light); ST, standard local time; LD, light-dark cycle; LL, constant dim light.

RESULTS

Correlation of Cell Shape and the Rhythm in Photosynthetic Capacity. When *Euglena gracilis* cultures are synchronized by a repetitive light-dark cycle, photosynthetic capacity oscillates in a predictable manner (Fig. 1B and Ref. 25). The capacity to evolve O_2 rises to a maximum at midday and then decreases until the next morning. The pattern persists for at least five 24-h cycles in constant dim light and has been previously characterized as circadian (25). If cells are examined microscopically at the times photosynthetic measurements are made, the shape of the cell can be correlated with the photosynthetic capacity. At those times when photosynthetic capacity is lowest (*e.g.* Fig. 1, CT 00, CT 24), the cell population consists predominantly of round cells (Fig. 1A). As photosynthetic capacity increases, the cells in the population increase in length, and when the cells have the greatest photosynthetic capacity (*e.g.* Fig. 1, CT 06, CT 30), at least 60 to 75% of the cells in the population are elongated. The population returns to round cells as the photosynthetic capacity decreases after its maximum. A difference in cell length at these two times of day can be noted by visual examination.

The characteristics of these shape changes can be studied by plotting the lengths of the cells in the population *versus* the cell number for each length. A summary of shape changes occurring during 12 h of a LD cycle is presented in Figure 2. Data from eight separate experiments are presented. The times represent 1 h before dawn (0800), three samples from the light period (1100, 1400, 1600), and 1 h after darkness (2000). At each time point, the average of the means for eight experiments (representing approximately 1500 cell length measurements) is given with SE. The mean cell length for the population changes in a predictable manner being lowest at the times when photosynthetic capacity is low (22 μm at ST 0800), highest when photosynthetic capacity is highest (30 μm at ST 1400) and then decreasing by ST 1700 and ST 2000 as photosynthetic capacity diminishes. In addition, the pattern of dispersion about the mean changes throughout the day, being skewed toward the smaller cell sizes at the beginning of the light portion of the cycle (ST 0800), returning to a more even distribution by ST 1400, and then becoming skewed again toward the smaller cell sizes after the maximum. When several populations are used for the calculation of mean cell size, the standard errors are small and differences in mean cell length are noticeable measuring a small interreplication variation. If individual experiments are examined, the mean length for the population changes with the same rhythmic pattern, but the length standard deviations, are large, indicating a large intrareplication variation. For example, in Figure 5, the mean cell length and SD were 26 ± 7 μm at the beginning of the light cycle (CT 00) and increased to 30 ± 8 μm in midday (CT 05). Because of the large standard deviations within any one experiment, a method other than the comparison of the population mean was devised to determine the significance of length changes within a single population. The skewedness of the population about the mean was quantitated by determining the percentage of the population occupying three decades of cell lengths: 15 to 24, 25 to 34, and 35 to 44 μm. The cells in the size range 15 to 44 μm represent approximately 98% of each population. Table I shows the distributions in each class as a function of standard time. The changes in cell length can most easily be understood by following the shortest and longest size classes. Significant differences in the populations were determined by comparing the percentage of cells in one size class with the percentage at any other time within the same size class. At ST

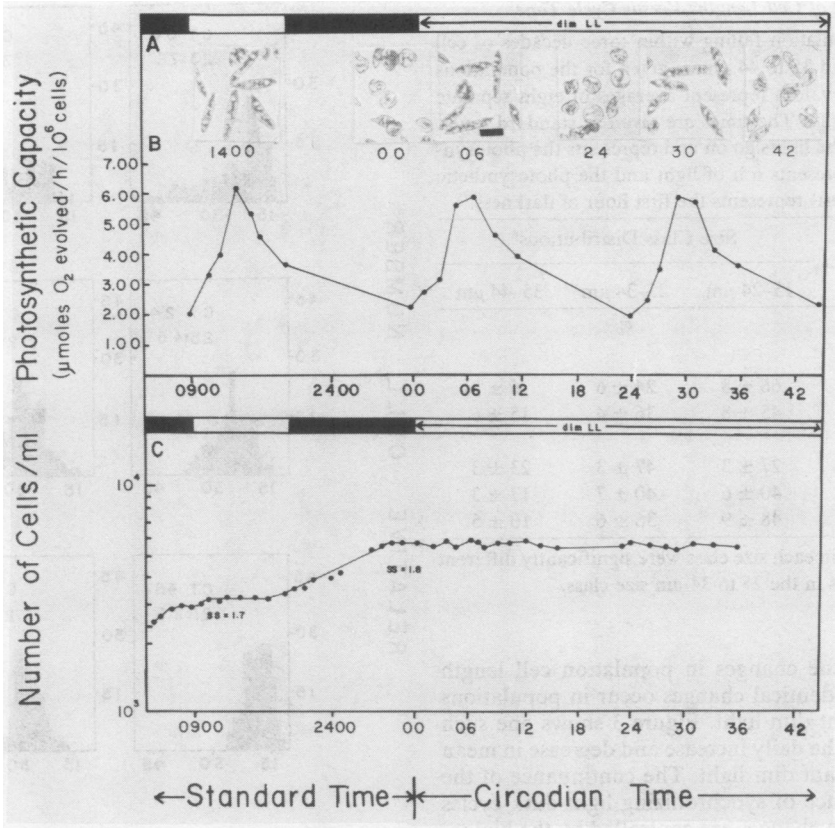

FIG. 1. Cell shape changes, photosynthetic capacity, and cell number as a function of standard and circadian time. A, Photomicrographs of cells at the minimum (ST 0900, CT 00, 24) and the maximum (ST 1400, CT 06, 32) of the photosynthetic rhythm. Bar represents 20 μm. B, Photosynthetic capacity rhythm of cells grown in repetitive cycles of 10-h light plus 14-h dark and then placed in constant dim light at CT 00 which represents the normal dawn. Lights came on at 0900 standard time (9 AM) and were turned off at 1900 (7 PM). Photosynthetic capacity is plotted as the rate of O_2 evolution. C, Cell number, same growth conditions as B. Cell number is nearly constant during the light portion of the cycle and approximately doubles by the end of the dark period. SS represents the step size or the number of cells after a period of cell division/number of cells before the division. A value of 2 would represent every cell dividing.

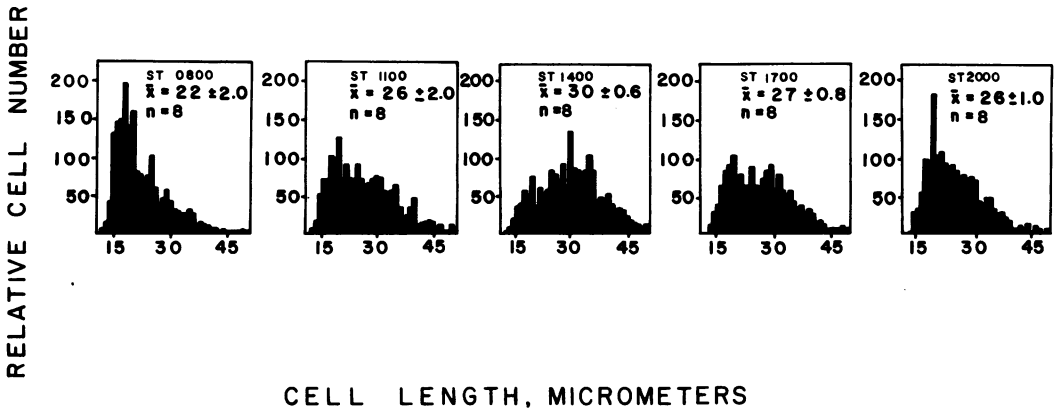

FIG. 2. Cell shape rhythm during a light-dark cycle. The cell lengths for eight separate experiments were plotted together. Times are given as ST with 0900 representing the beginning of the 10-h light period. ST 1400 represents the timing of the photosynthetic maximum of the population. $\bar{X}$ represents the average of the eight population means and the ± values are SEM.

0800, which represents 1 h before the dawn of a 10-h light, 14-h dark cycle, 66% of the eight cell populations had cell lengths between 15 and 24 μm. Only 6% of the populations had cells 35 to 44 μm long. After 2-h light (ST 1100), 45% of the cells are found in the smaller size class (a significant difference from ST 0800) while the percentage of the population in the longest size class has doubled to 15% (a significant difference from ST 0800). By ST 1400, which represents the photosynthetic maximum of the populations, the percentage of cells 15 to 24 μm long is lowest at 27% (a significant difference from ST 1100) while the percentage of cells 35 to 44 μm long is the greatest at 23% (a significant increase from ST 1100). Cells in the population begin to shorten after the photosynthetic maximum has passed and the percentage of cells 35 to 44 μm long steadily decreases as the percentage of cells 15 to 24 μm steadily increases. Six h after the photosynthetic maximum (ST 2000), only 10% of the population consists of the longest cells (a significant decrease from ST 1400) while 48% of the population is composed of cells 15 to 24 μm long (a significant increase from ST 1400). After 24 h, the population returns to the distribution shown at ST 0800 (data not shown for this figure, but

Table I. *Distribution of Cell Lengths Versus Cycle Time*

The percentage of the population falling within three decades of cell lengths, 15 to 24, 25 to 34, and 35 to 44 μm, is given for the populations represented in Figure 2. The values represent averages of eight separate means and the ± values are SEM. The times are given as standard times. ST 0800 (8 AM) is 1 h before the lights go on and represents the photosynthetic minimum. ST 1400 represents 6 h of light and the photosynthetic maximum, while ST 2000 (8 PM) represents the first hour of darkness.

Standard Time	Size Class Distributions[a]		
	15–24 μm	25–34 μm	35–44 μm
		%	
ST 0800 (photosynthetic minimum)	66 ± 8	24 ± 6	6 ± 2
ST 1100	45 ± 8	36 ± 4	15 ± 6
ST 1400 (photosynthetic maximum)	27 ± 3	47 ± 3	23 ± 3
ST 1700	40 ± 6	40 ± 7	17 ± 3
ST 2000	48 ± 9	36 ± 6	10 ± 5

[a] All adjacent vertical pairs in each size class were significantly different except the last two percentages in the 25 to 34-μm size class.

see Figs. 4–6).

While Figure 2 shows the changes in population cell length during a light-dark cycle, identical changes occur in populations maintained in 24-h constant dim light. Figure 3 shows one such population which displays the daily increase and decrease in mean cell length for 3 d in constant dim light. The continuance of the shape changes in the absence of synchronizing light-dark cycles indicates that the cell length changes are controlled by the biological clock. The rhythm was not followed beyond 3 d and no other criteria to prove the circadian nature were performed (*e.g.* phase shiftability, temperature compensation, etc.). Only populations from the maxima and minima of the cell shape rhythms are shown for each day in Figure 3. The expression of the cell shape rhythm in constant light conditions differs slightly from that seen with light-dark cycles (Fig. 2). The range (difference between the largest and smallest cell lengths) decreases with increasing exposure to the constant dim light. The cells in the population at CT 00 (beginning of the first day constant conditions) ranged between 14 and 50 μm in length with 65% of the population in the 15 to 24-μm size class and 14% in the 35 to 44-μm size class. The population at CT 72 (beginning of the fourth day constant conditions) ranged between 14 and 29 μm with 82% of the population in the 15 to 24-μm size class and 0% in the 35 to 44-μm size class. The percentage changes in both size classes represent significant shifts in the population. A similar trend is seen for the population dispersion at the daily maximum of the rhythm (CT 06, CT 30, CT 54). At CT 06 (the maximum of the first day), 27% of the population was in the 15 to 24-μm size class and 38% in the 35 to 44-μm size class. Three d later at CT 54, 30% of the population was in the 15 to 24-μm size class (no significant difference from CT 06), but 0% of the cells was in the 35 to 44-μm size class (significant difference from CT 06). Each successive day, the range of cell lengths at the rhythm maximum decreased, with fewer cells being found in the longest size class (35–44 μm) and more cells in the intermediate size class (25–34 μm). The percentage of cells in the smallest size class did not significantly change at the daily maximum.

Cell Volume. The volume of *Euglena* cells can be estimated from photographic measurements, provided the cells closely approximate any of the shapes for which volume equations can be easily applied. Such equations are available for cells exhibiting the two shape extremes, round (or spherical) and elongated (prolate spheroid or cigar-shaped). In view of a report of rhythmic volume changes in *Euglena* cultures (17), the volumes of the smallest cells at the beginning of the cycle (ST 0800) and those of the longest cells in the 45 to 50-μm length class at ST 1400 cell were determined. If a daily rhythm in volume exists, the two greatest population extremes could be used to indicate the magnitude of the difference. The volumes for 50 spherical cells (ST 0800) was 2676 ± 877 μm^3 while the volume of 50 long cells (ST 1400) was 1979 ± 941 μm^3, indicating that the volume of the cells remained constant as the shape changed.

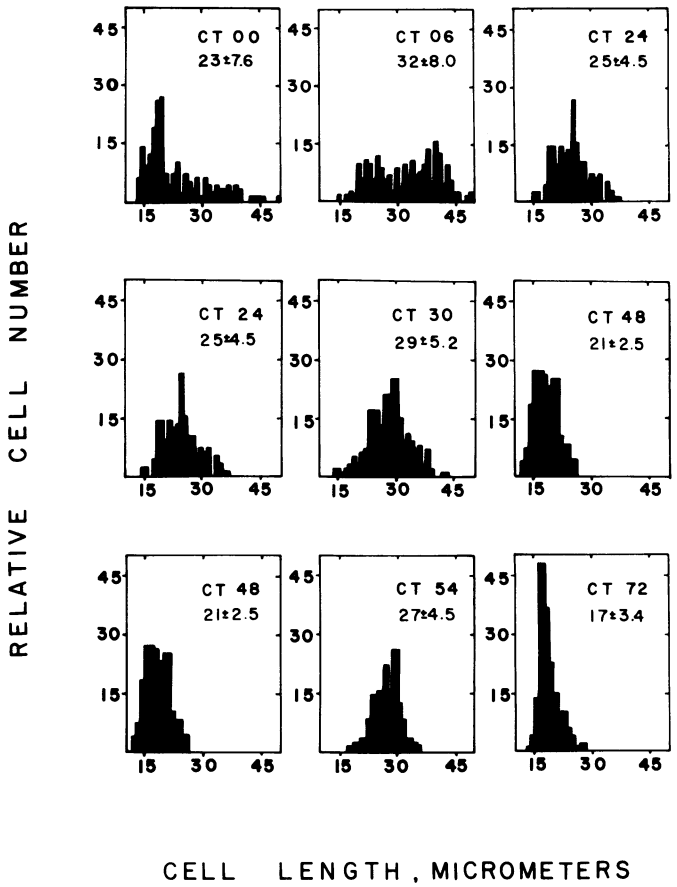

FIG. 3. Cell shape rhythm during constant dim light conditions. The cell lengths for a single experiment were plotted for three complete cycles in constant dim light (3.5 μE m^{-2} s^{-1}). Time is given in hours after the beginning of constant dim light (circadian time, CT 00) which began at the normal dark to light transition. The minima of the photosynthetic rhythm are represented by CT 00, 24, 48, and 72, while the maxima are represented by CT 06, 30, and 54. The mean cell length of each population is given ± SD.

Relation of the Cell Length Rhythm to Metaboly. Metaboly is a complex set of movements and shape transitions exhibited by euglenoids (2). One characteristic form of metaboly is the rapid (within seconds) transition from a round to an elongated shape. Microscopic observations of living populations were performed to determine the relationship between the rhythm in cell shape and metaboly. Regardless of when populations were examined, only those cells greater than 30-μm length exhibit metaboly. In addition, not all of the cells greater than 30 μm participated in metaboly. It appeared that certain long cells were very active in the metaboly shape changes while other cells of the same length did not alter their shape over the typical 30-min observation period. Because the percentage of cells 30 μm or longer changes with the time of day (Table I), the percentage of cells capable of participating in metaboly will change. The fact that the round cells were never observed to participate in metaboly movements suggests that the rhythm in cell shape is not the same as the

metaboly shape changes.

Separation of Cell Shape Changes from the Cell Cycle. The changes reported for cell length and volume might be related causally to the cell cycle if the cells are grown in LD cycles. It has been established that the cell cycle is influenced by the biological clock in *Euglena*, and that cell divisions occur by binary fission during the dark (13, 14). The decrease in mean cell length (Fig. 2) significantly precedes the timing of cell division which occurs predominantly during the dark portion of the LD cycle (Fig. 1). It is possible that a decrease in cell length might be a signal for the onset of mitosis. When cultures are placed in constant dim light, however, the rhythm in cell division ceases, at least for the duration of measurements reported here (Fig. 1), while the rhythm in cell length continues.

Effects of Inhibitors of Energy Metabolism on Cell Shape Changes. The intent of this investigation is to determine whether the cell shape changes require energy, and if so, to determine the pathways involved. The requirement for oxidative and/or photophosphorylation for the two shape changes was examined by testing the effect of several inhibitors of these pathways on the shape changes. The experimental design was the same for all experiments. Cultures were synchronized by growth for several days in a 10:14 (L:D) cycle. The beginning time of experimentation is called CT 00 and represents dawn (lights on) and the beginning of exposure to 48 h of constant dim light. At five times during the first day, cells were photographed and the data were plotted in histogram form. In all figures, this first day is presented as the top row and is a control to which other treatments are compared. At CT 24 (24 h after CT 00), the culture was divided equally into two halves. Cells from one flask were photographed at CT 24 and then inhibitor was added. Cells were examined 2 and 5 h after the inhibitor was added (CT 26 and CT 29, respectively) and the effect of the inhibitor on the transition from round to long shape was documented. These data are presented in the second row of all figures. No inhibitor was added to the other half of the culture until CT 29 when the cells were the longest. Photographs of the cells were taken at CT 29 before inhibitor was added and the cell response was recorded at 3 and 7 h after inhibitor addition (CT 32 and CT 36, respectively). The effect of the inhibitor on the transition from long shape back to round was examined in this instance. These data are presented in the third row of all figures.

The ATP requirement for the two cell shape changes occurring each 24-h period was initially investigated by uncoupling oxidative and photophosphorylation with gramicidin D (Fig. 4). Gramicidin added at CT 24 (second row) resulted in a complete blockage of elongation. The percentage of the cells in each size class is not statistically different between the population at CT 24 (when the inhibitor was added to one-half of the control culture) and the population at CT 29 representing a 5-h exposure to gramicidin. When gramicidin was added to the other half of the culture at CT 29 (third row), a complete blockage of the long to round transition was observed, and the CT 36 population (7-h exposure) was not significantly different from the CT 29 population (time of gramicidin addition). The gramicidin concentrations used resulted in a maximal stimulation of light-induced electron flow using a H_2O to MV reaction performed with whole cells at the photosynthetic maximum (26). However, a higher concentration was required to uncouple at CT 24 (20 μM gramicidin) than at CT 29 (10 μM gramicidin).

When NaN_3 is added to round cells at CT 24 (2 mM final concentration), a complete blockage of elongation is observed (Fig. 5, second row). After a 5-h exposure to NaN_3 (CT 29), 72% of the cells remain in the 15 to 24-μm size class as compared to the 32% in the control at CT 05, while 0.4% of the cells are found in the 35 to 44-μm size class compared to the 19% for the control. The 2 mM NaN_3 inhibited O_2 consumption 100%, as measured with an O_2 electrode, while photosynthesis measurements of O_2 evolution were normal. NaN_3 (1 mM final concentration) added at CT 29 (Fig. 5, third row) blocked the transition of the elongated cells back to round cells (compare CT 36 to control at CT 12). After 7 h of 1 mM NaN_3, only 30% of the cells were in the 15 to 24-μm size class compared to the 59% in the control, and 29% of the population was in the longest size class as compared to the 5% for the control. The 1 mM NaN_3 added at CT 29 inhibited O_2 consumption 100% and did not affect O_2 evolution. The inhibitor added at CT 24 completely inhibited the cell shape change and respiration only if added at a concentration of 2 mM or greater. However, 1 mM NaN_3 was very effective by CT 29, indicating that the cells had different sensitivities to this inhibitor, as with gramicidin, depending on the time of day added (see "Discussion").

Antimycin A also blocked both the round to long and the long to round transitions (data not shown). As with NaN_3 and gramicidin, a higher concentration was required to completely block respiration and the shape transition when added at CT 24 (200 μM) while the lower concentration of 100 μM antimycin was effective when added at CT 29.

The use of KCN gave inconclusive results. It is likely that the rapid aeration of the cultures resulted in the release of HCN from the culture, thus lowering the effective concentration of CN^- in the culture (37).

The involvement of noncyclic photophosphorylation was tested by adding 5 μM DCMU in DMSO (0.1% [v/v] final concentration DMSO) at CT 24 (Fig. 6, second row) and CT 29 (Fig. 6, third row). After a 5-h exposure to DCMU (CT 29), 64% of the cells remain in the 15 to 25-μm size class as compared to 30% in the control at CT 05, while 5% of the cells are found in the 35 to 44-μm size class compared to the 20% for the control. When added at CT 29, the maximum of the photosynthetic capacity rhythm, no effect was observed on the transition from elongated back to round. No O_2 evolution was measured in the presence of DCMU, while normal rates of respiration were detected.

The presence of atrazine (10 μM final concentration) caused the same results as reported for DCMU (data not shown).

Effects of Cytoskeletal Inhibitors on the Cell Shape and Photosynthetic Rhythms. The effects of arresting or altering the daily rhythm in cell shape was investigated by the addition of cytoskeletal inhibitors. Cytochalasin, which is thought to alter actin monomers (5), was used to investigate the possible involvement of microfilaments in the photosynthetic and cell shape rhythms. At various times during the 24-h cycle, the cell shape profile and photosynthetic capacity were determined in addition to the construction of light intensity plots. Photosynthetic capacity was measured 7 times/24-h cycle, cell shape profile three times, and light intensity plots twice. Times at which two or more parameters were simultaneously measured are referenced in the figures by letters. Figure 7, A and B, shows the relationship between cell shape and photosynthetic capacity before and after the addition of 100 μM cytochalasin B or cytochalasin D. The rhythm in cell shape is demonstrated in Figure 7A (control times a–d) and the rhythm of photosynthetic capacity in Figure 7B (control times a–d). The population cell shape profile throughout the LD cycle (positions a, b, and c) shows the same trend as the controls in Figures 4 to 6. At d, 100 μM cytochalasin B was added to the culture (Fig. 7B, arrow). The effect of cytochalasin on the cell shape profile was followed for the next 24 h while the effect on photosynthetic capacity was followed for 36 h. The population profile did not substantially change in the 24 h following the addition of the inhibitor (Fig. 7A, times d–g), with the greatest percentage of cells found in the 15 to 24-μm size class and only 3 to 9% of the cells in the longest 35 to 44-μm size class. The rhythm of cell shape changes is thus abolished by the addition of cytochalasin.

The effect of cytochalasin on the rhythm in photosynthetic capacity is shown in Figure 7B. While the oscillation in the rate

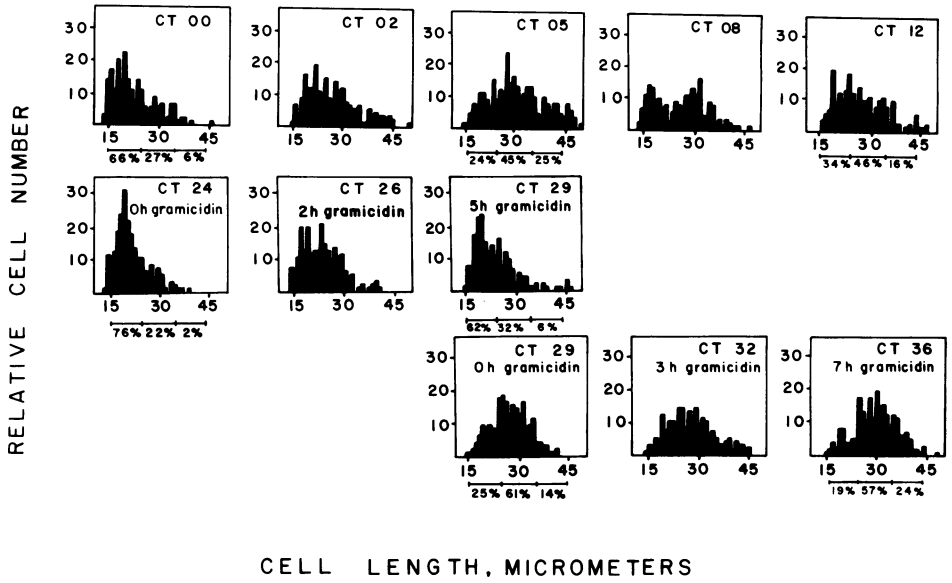

FIG. 4. The effect of gramicidin D on cell length. Top row: control day 1. The culture was divided into two aliquots at CT 24. Middle row: at CT 24, 20 μM gramicidin D (final concentration, dissolved in DMSO, 0.1% [v/v] final concentration) was added to one aliquot and cell length was followed in the population at CT 26 (2-h exposure) and CT 29 (5-h exposure). Bottom row: at CT 29, 10 μM gramicidin D (final concentration) was added to the second aliquot and cell length was followed in the population at CT 32 (3-h exposure) and CT 36 (7-h exposure). The percentages represent the proportions of the population found in the size classes 15 to 24, 25 to 34, and 35 to 44-μm length.

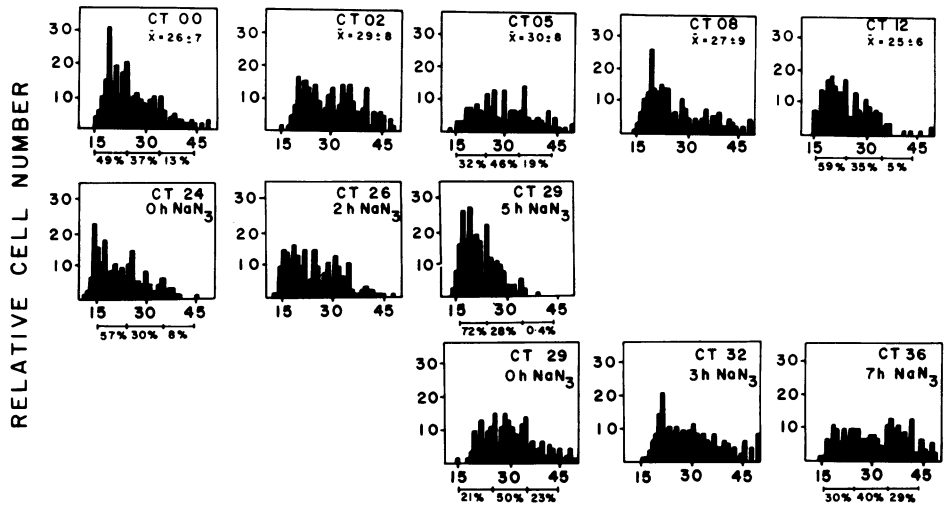

FIG. 5. The effect of sodium azide on cell length. Top row: control, day 1. The cell lengths of the culture are plotted as a function of time. $\bar{X}$ represents the mean of the population, the $\pm$ values are SD, and n is the individual population size for each time point. The culture was divided into two aliquots at CT 24. Middle row: at CT 24, 2 mM NaN_3 (final concentration) was added to one aliquot and cell length was followed in the population at CT 26 (2-h exposure) and CT 29 (5-h exposure). Bottom row: at CT 29, 1 mM NaN_3 (final concentration) was added to the second aliquot and cell length was followed in the population at CT 32 (3-h exposure) and CT 36 (7-h exposure). The percentages represent the proportions of the population found in the size classes 15 to 24, 25 to 34, and 35 to 44-μm length.

of O_2 evolution continues for the two subsequent LD cycles examined, the shape of the curve is altered in the presence of cytochalasin. The amplitude of the rhythm decreases while the peak at the maximum is broader.

There are two obvious explanations for the modification of the O_2 evolution rhythm observed in the presence of cytochalasin. One is that the photosynthetic capacity rhythm involves a change in cell shape caused by microfilaments. Disruption of microfilament polymerization by cytochalasin would thus be predicted to alter the expression of the photosynthetic capacity rhythm. The second alternative is that cytochalasin causes other cytotoxic effects that are not related to microfilament integrity. Because the pattern of O_2 evolution appeared to be affected, the most logical site of secondary action for cytochalasin would be the light reactions.

Two methods were used to investigate whether cytochalasin alters the light reactions. The first method involved an analysis of light intensity plots. When the rate of O_2 evolution is determined at successively increased light intensities (below the saturating light intensity) and plotted as light intensity/rate of O_2 evolution *versus* light intensity, the slope of the line is an indication of the light reaction efficiency. It has previously been demonstrated for

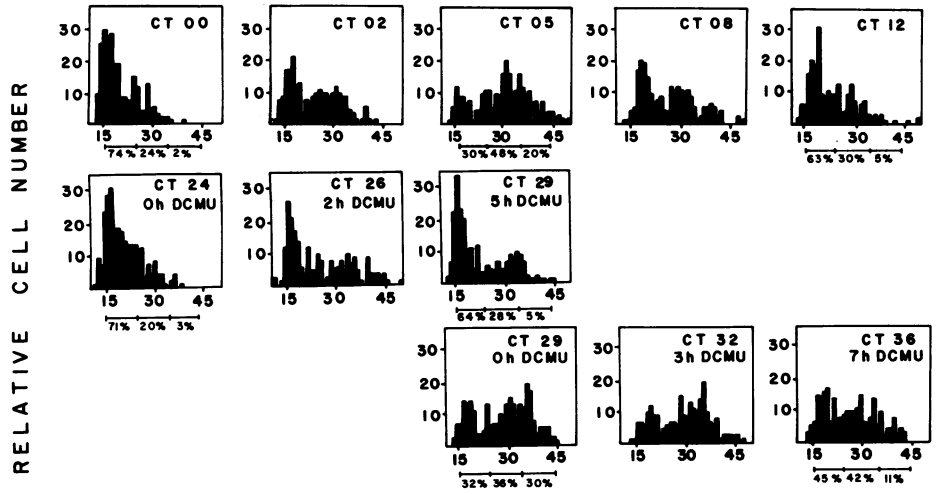

FIG. 6. The effect of DCMU on cell length. Top row: control, day 1. The culture was divided into two aliquots at CT 24. Middle row: at CT 24, 5 μM DCMU (final concentration, dissolved in DMSO, 0.1% [v/v/cb final concentration) was added to one aliquot and cell length was followed in the population at CT 26 (2-h exposure) and CT 29 (5-h exposure). Bottom row: at CT 29, 5 μM DCMU (final concentration) was added to the second aliquot and cell length was followed in the population at CT 32 (3-h exposure) and CT 36 (7-h exposure). The percentages represent the proportions of the population found in the size classes 15 to 24, 25 to 34, and 35 to 44-μm length.

Euglena (26) that, when such measurements are made at several times during the 24-h cycle, the relative slopes of the light intensity plots can be predicted from the time point within the LD cycle that measurements are performed. Light intensity plots constructed at the photosynthetic minimum (Fig. 7C, line a) and the photosynthetic maximum (Fig. 7C, line b) have different slopes. The difference in slope at the two times of day represents a difference in the ability of the cells to absorb and/or process the incident light. Line d (Fig. 7C) is the light intensity plot measured just prior to the addition of cytochalasin while line e corresponds to time e on the photosynthetic capacity curve which is 5 h after the addition of the inhibitor. The expected relative positions of the two lines obtained at the photosynthetic minimum and maximum have not been altered by the presence of cytochalasin: the slope of line e is lower than the slope of line d, an observation which indicates a faster rate of O_2 evolution at each light intensity for the afternoon population. Lines g and h were measured at the photosynthetic minimum (time g) and maximum (time h) of the second day of exposure to cytochalasin, with line g representing 24-h exposure to the inhibitor and line h representing 29-h exposure. No alteration in the respective slopes measured at the photosynthetic minimum and maximum was observed after 1-d exposure to cytochalasin.

Although no inhibitory effects of cytochalasin were observed on the *in vivo* assay of O_2 evolution, an *in vitro* assay was used to document this observation. The possible inhibition by cytochalasin of light-induced electron flow rates was measured with chloroplasts isolated from *Euglena* cells 2 h after the onset of the illumination cycle. The chloroplasts were divided into aliquots, one being incubated with 100 μM cytochalasin B, another with cytochalasin D. The rate of noncyclic electron flow, as measured with a H_2O to MV assay in the presence of gramicidin, was determined at the time of isolation and after a 5-h treatment. Table I indicates that chloroplasts do not respond to the two cytochalasins in an identical manner. The rate of light-induced electron flow was initially inhibited 4% by the addition of cytochalasin B, and was inhibited 6% by cytochalasin D. Five h later, the rate of light-induced electron flow was inhibited an average of 6% by cytochalasin B but was inhibited 28% by cytochalasin D.

Identical experiments were performed with colchicine, an inhibitor of microtubule polymerization, and lumicolchicine, a derivative that does not effect polymerization (Fig. 8). The cell populations presented in Figure 8 exhibit the typical daily change in cell shape as shown in Figure 8A, times a, b, and c. At time d (the dark to light transition of the second cycle), either 2.5 mM colchicine or lumicolchicine was added to the culture. Colchicine prevented the population cell shape profile from changing over the subsequent 24 h. Times e, f, and g of Figure 8A indicate that the percentage of cells in the 15 to 24-μm size class remains high during exposure to colchicine while the percentages of cells in the 25 to 34- and 35 to 44-μm size classes remains low. Thus, colchicine effectively blocks the rhythmic change from round to elongated cells. Lumicolchicine, however, had no noticeable effect on the transition of the cell population from spherical cells to elongated cells (Fig. 8A, times d–f).

The effect of colchicine on *in vivo* O_2 evolution is rather dramatic (Fig. 8B). The rhythm in O_2 evolution is dampened regardless of whether the colchicine is added at the beginning of the light cycle (photosynthetic minimum, time d) or at the photosynthetic maximum (data not shown). There was no reproducible effect of lumicolchicine on the expression of the photosynthetic capacity when followed for the light portion of the LD cycle (Fig. 8B). The effect of lumicolchicine for extended time periods was not studied.

The possibility that colchicine or lumicolchicine alters the photosynthetic light reactions was tested *in vivo* by examining the effect on light intensity plots and *in vitro* by the effect on the rate of light-induced electron flow. Figure 8C indicates the effects of colchicine on light intensity plots. Lines a and b, representing the photosynthetic minimum and maximum, respectively, of the first cycle, show the typical pattern. Line d represents the data obtained at the time just prior to the addition of colchicine, while line e was constructed from data collected after a 5-h exposure to the inhibitor. The typical difference in relative slope between the two times of day (beginning of the light cycle and middle of the light cycle) was not observed, with the two slopes being very similar. If colchicine has no effect on the O_2 evolution process, line e would be predicted to have a smaller relative slope than line d measured 5 h earlier. Lumicolchicine had no such effect on the slopes of the light intensity plots (Fig. 8C, lines d and e).

Further evidence that colchicine affects the photosynthetic reactions was observed with isolated chloroplasts. Table II indicates that colchicine caused no initial inhibition of light-induced elec-

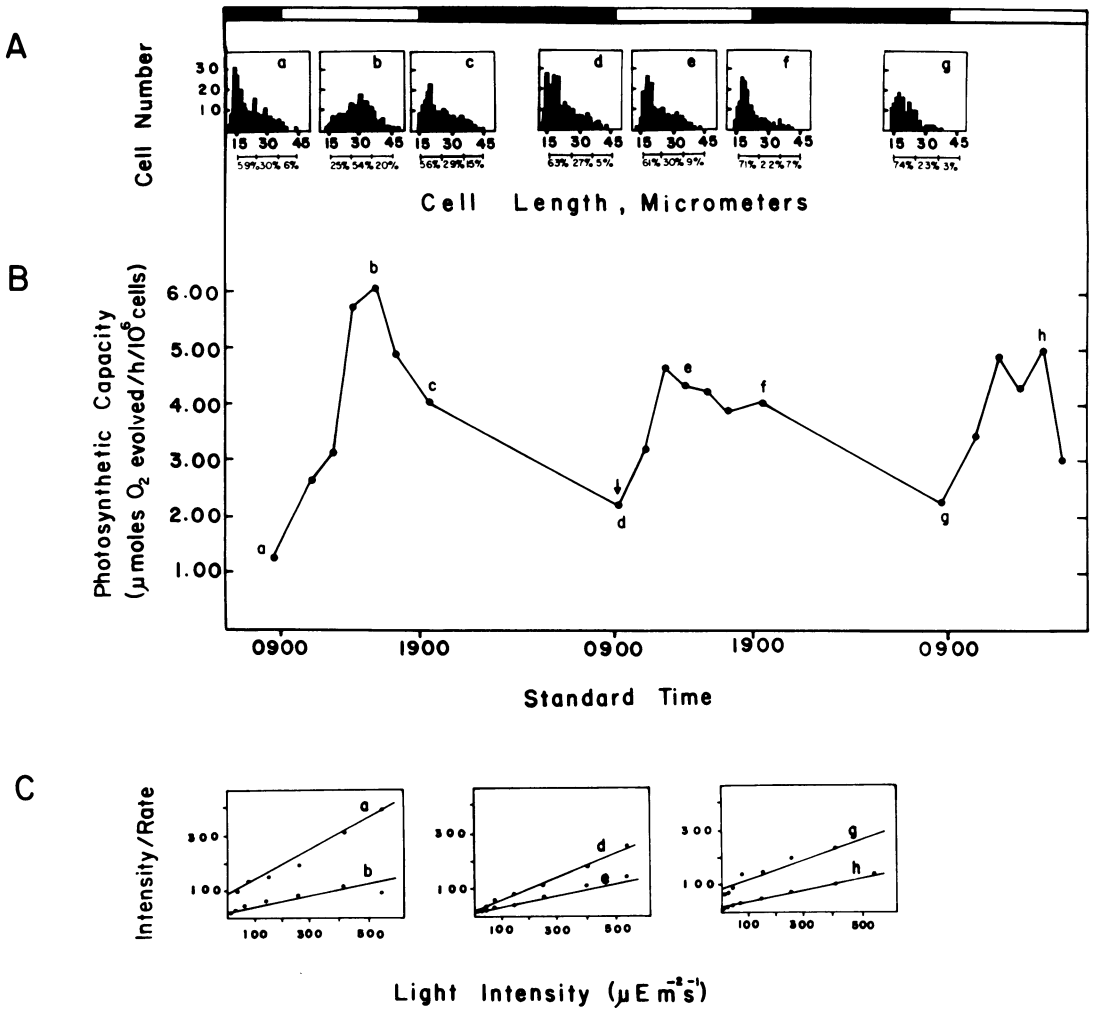

FIG. 7. Effect of cytochalasin on the cell shape and photosynthetic capacity rhythms. A, Effects of 100 μM cytochalasin B on cell shape. Open bars at the top represent the 10 h light in the LD cycle from 0900 (9 AM) to 1900 (7 PM); dark bars represent the 14 h dark in the LD cycle from 1900 (7 PM) to 0900 (9 AM). Cells were removed from the culture seven times and cell lengths were measured and plotted in histogram form. Letters a to g correspond to the times on the photosynthetic capacity curve given in B. Time a is just prior to the dark to light transition, b is the middle of the light period, c represents the light to dark transition, and d is the dark to light transition of the next cycle (24 h after a). Points a to d represent the control values for those times. At the time represented by d, 100 μM cytochalasin was added. Time e represents 5-h exposure to cytochalasin (middle of the light period), f represents 11-h exposure to cytochalasin (light to dark transition), and g represents 24-h exposure (dark to light transition of the third cycle). The percentage of each population in the size classes 15 to 24, 25 to 34, and 35 to 44-μm cell length is given. B, Effect of cytochalasin on the O_2 evolution rhythm. Letters correspond to the times cells were removed from the culture for cell shape measurements (given in A) or light intensity plots (given in C). Points a to d represent the control cycle showing the typical shape of the photosynthetic capacity rhythm. At the arrow (point d), cytochalasin was added to the culture and O_2 evolution rates were followed for one and one-half cycles of LD. C, Effect of cytochalasin on the slope of light intensity plots. Line a was constructed from cells removed at the photosynthetic minimum of the first cycle (time a in B) while line b was constructed from cells removed at the photosynthetic maximum of the first cycle time b in B). The slope differences of this control are characteristic of the minimum and maximum photosynthetic capacities. Line d was constructed from measurements at the photosynthetic minimum of the second cycle (point d in B) and the time of cytochalasin addition, and e was constructed at the photosynthetic maximum of the second cycle and represents 5-h exposure to cytochalasin (point e in B). Line g represents 24-h exposure to cytochalasin and represents the photosynthetic minimum of the third cycle (point g in B) whereas line h represents 29-h exposure to cytochalasin and represents the photosynthetic maximum of the third cycle (point h in B).

tron flow. A 5-h incubation, however, resulted in a 62% inhibition of the electron flow rate when compared to the controls measured 5 h after isolation. The effect of colchicine on the photosynthetic rhythm could therefore be attributed to an inhibition in the rate of light-induced electron flow.

Although no effects of lumicolchicine were observed for the photosynthetic capacity rhythm or the daily change in the slopes of light-intensity plots, an average inhibition of 43% in the rate of light-induced electron flow was observed with isolated chloroplasts (Table II).

Demecolcine (Colcemid), a derivative of colchicine, was ineffective at altering cell shape in the early hours of the light cycle up to a concentration of 5 mM (the highest concentration tested). Demecolcine was found to inhibit the rate of light-induced electron flow by 61% after a 5-h incubation in the chloroplast system (Table II).

DISCUSSION

Two general approaches have been utilized to study the possible relationship between the cell shape and photosynthetic rhythms reported for *Euglena* (Figs. 1–3). This investigation attempts to determine whether the rhythm in cell shape is dependent upon the photosynthetic and respiratory pathways for an energy supply

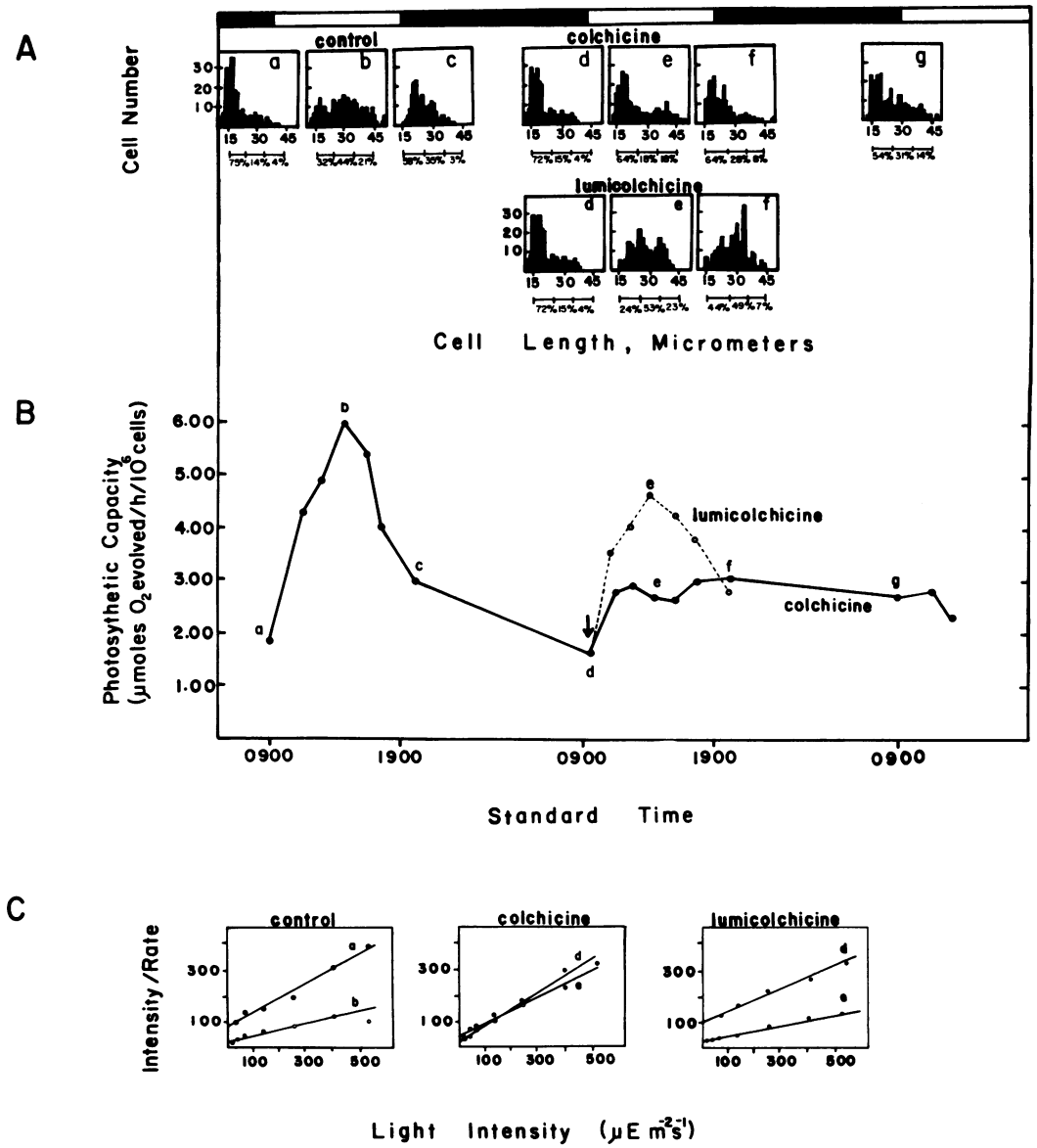

FIG. 8. Effect of colchicine and lumicolchicine on the cell shape and photosynthetic capacity rhythms. A, Effect of 2.5 mM colchicine or lumicolchicine on cell shape. Open bars at the top represent the 10 h light in the LD cycle from 0900 (9 AM) to 1900 (7 PM), and dark bars represent the 14 h dark in the LD cycles from 1900 (7 PM) to 0900 (9 AM). Cells were removed from the culture seven times and cell lengths were measured and plotted in histogram form. Letters a to g correspond to the times on the photosynthetic capacity curve given in B. Time a is just prior to the dark to light transition, b is the middle of the light period, c is the light to dark transition, and d is the dark to light transition of the next cycle (24 h after a). Points a to d represent the control values for those times. At time d, 2.5 mM colchicine or lumicolchicine was added to the culture. Time e represents 5-h exposure to colchicine or lumicolchicine (middle of the light period), f represents 11-h exposure (light to dark transition), and g represents 24-h exposure (dark to light transition of the third cycle). The percentage of each population in the size classes 15 to 24, 25 to 34, and 35 to 44-μm cell length is given. B, Effect of colchicine and lumicolchicine on the O_2 evolution rhythm. Letters correspond to the times cells were removed from the culture for cell shape measurements (given in A) or light intensity plots (given in C). Points a to d represent the control cycle showing the typical shape of the photosynthetic capacity rhythm. At the arrow, point d, 2.5 mM colchicine or lumicolchicine was added to one culture at the photosynthetic minimum and O_2 evolution rates were followed for one and one-half cycles of LD. C, Effect of colchicine and lumicolchicine on the slope of light intensity plots. Line a was constructed from cells removed at the photosynthetic minimum of the first cycle (time a in B) whereas line b was constructed at the photosynthetic maximum of the first cycle (time b in B) and the time of colchicine or lumicolchicine addition to the culture. Line e was constructed at the photosynthetic maximum of the second cycle and represents 5-h exposure to colchicine or lumicolchicine.

and if the photosynthetic rhythm is influenced by the shape of the cell.

The daily changes in the shape of *Euglena* persist for at least 3 d in constant dim light (Fig. 3). The rhythmic changes in cell shape can tentatively be classified as a circadian rhythm because (a) the phenomenon is rhythmic and repeats itself approximately every 24 h and (b) the rhythm persists or repeats in the absence of environmental cues (*e.g.* LD cycles). The exact period length of the rhythm has not been determined. The rhythms discussed in this report—cell shape and photosynthetic capacity—can both be dissociated from the cell cycle-related division known to occur in LD cycles or constant darkness. The biological clock-related cell division rhythm that has been highly characterized (13, 14) does not persist in the constant dim light conditions utilized in this study (Fig. 1).

The energy requirements for accomplishing the two daily cell

Table II. *The Effect of Cytochalasin, Colchicine, and Lumicolchicine on the Rate of Light-Induced Electron Flow*

Chloroplasts were isolated from a culture 2 h into the light portion of a LD cycle. The rate of a H_2O to MV assay, in the presence of gramicidin, was measured immediately after the addition of inhibitor to aliquots of the chloroplast suspension (0 h measurements). Chloroplasts were incubated on ice for 5 h and rates remeasured. The percentage of inhibition was determined by comparing the experimental value to the control of the same incubation time. The ± values represent SE.

Treatment	Rate of Light-Induced Electron Flow		
	Time	H_2O to MV assay	Inhibition of rate
	h	*μmol O_2 consumed h^{-1} mg^{-1} Chl*	%
Control rate	0	20.1 ± 1.2	
	5	15.9 ± 1.4	
Cytochalasin B	0	19.4 ± 2.3	4
100 μM	5	14.9 ± 2.0	6
Cytochalasin D	0	18.9 ± 0.9	6
100 μM	5	11.5 ± 0.8	28
Colchicine	0	20.9 ± 0.8	0
2.5 mM	5	7.7 ± 1.6	62
Lumicolchicine	0	17.5 ± 1.3	13
2.5 mM	5	9.0 ± 2.0	43
Demecolcine	0	18.9 ± 2.7	6
2.5 mM	5	7.8 ± 1.9	61

shape changes were investigated by exposing cells to various metabolic inhibitors that presumably inhibit specific biochemical reactions. The investigation of whether ATP or a high energy state of mitochondrial and/or chloroplast membrane systems is involved was initially performed with gramicidin D, an uncoupler of oxidative and photophosphorylation. The presence of gramicidin disrupted both shape transitions (Fig. 4), indicating that the round to long and the long to round shape changes both require the input of energy, presumably ATP. Thus, the long to round shape transition represents an energetic step and is not merely a relaxation from an energy-dependent elongated form. It appears from this study that the energy available to accomplish the shape changes is not stored and available to the cells, and that continuous production of ATP may be required.

The source of ATP production would most logically be predicted to be oxidative phosphorylation. Disruption of ATP production from the oxidative phosphorylation pathway was accomplished by inhibiting mitochondrial electron transport with NaN_3 and antimycin A. The presence of either of these inhibitors inhibited the round to long and the long to round shape transitions (Fig. 5). These results indicate that the ATP required for the two daily shape changes is derived predominantly from oxidative phosphorylation. These results do not discount the possibility that there may be an additional requirement for or utilization of ATP produced by the light reactions. However, if ATP from light-induced electron transport were utilized by the cells to change shape, the population would be expected to change lengths in the presence of the mitochondrial inhibitors, which did not occur. Antimycin A inhibits mitochondrial electron flow, but has also been implicated in the inhibition of cyclic photophosphorylation (3, 21, 35). Whether antimycin inhibits cyclic photophosphorylation in addition to oxidative phosphorylation was not investigated in this system.

When noncyclic light-induced electron flow is blocked in a population of spherical cells, the cells do not elongate (Fig. 6, middle row). Inhibition of noncyclic electron flow in a population of elongated cells (Fig. 6, bottom row), however, has no effect on the population transition back to the smaller, spherical cells. The observation that the long to round transition can occur in the absence of the photosynthetic capacity rhythm, which is inhibited by the presence of DCMU, indicates that the photosynthetic rhythm is not the direct cause of the shape change rhythm. The apparent lack of involvement of the photosynthetic reactions in the long to round transition could be explained by hypothesizing that, when the DCMU was added to the population of elongated cells at CT 29 (Fig. 6), the photosynthetic reactions had resulted in sufficient carbohydrate accumulation between CT 24 (photosynthetic minimum) and CT 29 (photosynthetic maximum) to provide substrate for oxidative phosphorylation. An analysis of carbohydrate reserves over the 24-h period would indicate if this hypothesis is realistic.

While the rhythm in cell shape is dependent upon the operation of the photosynthetic reactions for the round to long transition, it could also be asked whether the changes in cell shape affect the ability of the cells to absorb incident light effectively. Such a study would question whether the shape changes perform the same type of function as chloroplast orientation movements (7, 8). In an attempt to determine if there is any photosynthetic adaptive significance for the cell shape rhythm, cell shape was altered with cytoskeletal inhibitors that disrupt microfilaments and microtubules.

The inhibition of the naturally occurring shape changes by the addition of cytochalasin (Fig. 7A) implies that the two shape changes involve microfilaments. This conclusion, however, can only be made if cytochalasin is a specific inhibitor for altering microfilament integrity. Two different cytochalasins with different cytotoxic effects were used in this study because the specificity of this inhibitor has been questioned (5, 11, 23). The data presented in Figure 7 represent cytochalasin B. It has been reported that cytochalasin B inhibits the synthesis of ATP in isolated rat mitochondria (23) as well as glucose transport across rat cell plasma membranes (30). If cytochalasin blocks mitochondrial ATP production at the concentration used in the *Euglena* system, then the inhibition of cell shape changes presented in Figure 7A could be the result of disrupted oxidative phosphorylation which is necessary for the expression of the cell shape rhythm (Fig. 5). The effects of cytochalasin on mitochondrial activities was not investigated, but cytochalasin D, which does not inhibit membrane transport in rat cells (30), was also used with the hope of avoiding cytotoxic effects.

Both cytochalasins B and D altered the usual shape of the photosynthetic capacity (Fig. 7B), indicating either that this rhythm is dependent upon microfilaments for its expression or that the inhibitor alters the photosynthetic reactions. The presence of cytochalasin B did not alter the predicted daily change in the slope of the light intensity plots constructed from measurements obtained at the photosynthetic minimum and maximum of the rhythm (Fig. 7C). In addition, a 5-h chloroplast incubation with this inhibitor, representing a system not expected to have any microfilaments, only resulted in an average rate inhibition of 6% for the light-induced electron flow assay (Table II). Whether the 6% inhibition of electron flow rate measured *in vitro* is manifested *in vivo* as the broadening of the O_2 evolution rhythm (Fig. 7B) is unknown. The existence of a persistent rhythm in light-induced electron flow in a chloroplast system (26) indicates that some aspect of chloroplast biochemistry must be oscillating and is responsible for the primary expression of the rhythm in light reaction rates. It is possible, however, that the ultimate expression of the photosynthetic rhythm also involves a microfilament component such as the microfilament control of chloroplast orientation in *Mougeotia* (36) and *Funaria* (33).

While cytochalasin D also inhibited the cell shape changes and altered the photosynthetic capacity rhythm in the same manner as cytochalasin B, the rate of light-induced electron flow was in-

hibited an average of 28% (Table II). Unlike the mammalian system (30), cytochalasin B was therefore considered preferable to the D form in the *Euglena* system.

The possible involvement of microtubules in regulating the cell shape and photosynthetic rhythms was investigated by the addition of colchicine and lumicolchicine. Lumicolchicine, a mixture of colchicine isomers derived from UV irradiation, is thought to mimic many cytotoxic actions of colchicine but has no effect on microtubules. The addition of colchicine blocked both shape transitions, while lumicolchicine had no significant effect on cell shape (Fig. 8A). Colchicine also inhibited both the expression of the photosynthetic rhythm (Fig. 8B) and the daily change in the slope of light intensity plots (Fig. 8C). Lumicolchicine, however, did not cause any short term alteration in the photosynthetic rhythm (Fig. 8, B and C). The conclusion that the shape changes are dependent upon microtubules becomes clouded in view of the observation that colchicine inhibits light-induced electron flow rates an average of 62% in the isolated chloroplast system which would not be expected to have microtubules (Table II). Thus, the inhibition of the round to long shape change by colchicine may be the result of inhibiting photosynthesis which is necessary to accomplish the round to long shape transition (Fig. 6). The possible involvement of microtubules in the long to round shape transition is somewhat clearer. The long to round shape change is not dependent upon photosynthesis (Fig. 6) yet is inhibited by colchicine (data not shown). The effect of colchicine on photosynthesis can therefore be separated from its effect on shape changes during the long to round shape transition.

The validity of using lumicolchicine as a control in microtubule studies must be questioned in view of the results presented in Figure 8 and Table II. Even though lumicolchicine showed no measurable effect on the *in vivo* photosynthetic reactions, the rate of light-induced electron flow in the chloroplast system was inhibited 43% by the presence of lumicolchicine. The finding that lumicolchicine inhibits the photosynthetic reactions *in vitro* (Table II) but not *in vivo* (Fig. 8, B and C) implies that lumicolchicine may not be permeable across the *Euglena* plasma membrane. If lumicolchicine is not permeable, then no effects on cell shape or whole cell O_2 evolution would be expected. The use of broken chloroplasts (Class II) in the *in vitro* photosynthetic system would alleviate any permeability problems. The validity of using lumicolchicine as a control has been questioned on other grounds (32).

Demecolcine (Colcemid), an active derivative of colchicine, was inactive in altering cells shape even at high concentrations (5 mM), which also indicates a possible permeability problem for this inhibitor. While demecolcine might be more permeable if solubilized in DMSO, this approach was not investigated in light of the finding that demecolcine inhibited light-induced electron flow by 61% (Table II).

A more direct approach to determine the involvement of microfilaments and microtubules in these two rhythms is currently in progress. Using the technique of indirect immunofluorescence, a visualization of microtubule patterns throughout the daily cycle is underway, including studies using several inhibitors reported in this study.

An interesting observation from this study was the lower sensitivity of round cells to the inhibitors added at CT 24. Several of the inhibitors including NaN_3, gramicidin, antimycin, and colchicine, had to be added in higher concentrations at CT 24, as compared to addition at CT 29, in order to see a positive effect on the energy pathways and cell shape. This raises the question as to whether the membrane permeability in *Euglena* is rhythmic, being lower in the morning than in the afternoon. A rhythmic response to acid added to *Euglena* cells has been reported (6), and rhythms in membrane (9, 29) and transport phenomena (15, 19) are common in circadian rhythm studies. It is also possible that no rhythmic changes in permeability exist, but rather that respiration and photosynthesis are not equally sensitive to their inhibitors at various times of the day. Such a situation has been reported for uncouplers of photophosphorylation (24). Alternatively, the different sensitivity of the cells may be a reflection of a greater surface area/volume ratio in the elongated cells.

The use of chemical inhibitors to study biological clock-controlled processes has a major inherent problem. Although inhibitors like NaN_3 and gramicidin alter the ability of *Euglena* cells to change shape, the possibility always exists that the inhibitors directly alter the functioning of the clock itself. The possibility that the inhibitors NaN_3, antimycin, or gramicidin alter the clock was determined by monitoring the rhythm in O_2 evolution in cultures exposed to those inhibitors. During the short duration of the experiments (12 h), the O_2 evolution rhythm was not noticeably altered in the cultures exposed to the three inhibitors. Thus, if the inhibitors alter the biological clock, the response of the clock was not immediate. The inhibition of the cell shape changes observed within a few hours of exposure to the inhibitors is therefore attributed to the primary action of the inhibitors on respiration or photosynthesis and not an immediate effect on the clock.

Acknowledgment—I thank Dr. Sherwood Githens, III for helpful discussions during this work.

LITERATURE CITED

1. ARNON DI 1949 Copper enzymes is isolated chloroplasts. Polyphenoloxidase in *Beta vulgaris*. Plant Physiol 24: 1–15
2. ARNOTT HJ, PL WALNE 1966 Metaboly in *Euglena granulata*. J Phycol 2 (suppl): 4a (abstr)
3. BOHME H, S REIMER, A TREBST 1971 The effect of dibromothymoquinone, an antagonist of plastoquinone, on noncyclic and cyclic electron flow systems in isolated chloroplasts. Z Naturforsch 266: 341–352
4. BOUCK GB, DL BROWN 1973 Microtubule biogenesis and cell shape in *Ochromonas*. I. The distribution of cytoplasmic and mitotic microtubules. J Cell Biol 56: 340–359
5. BRADLEY MO 1973 Microfilaments and cytoplasmic streaming: inhibition of streaming with cytochalasin. J Cell Sci 12: 327–343
6. BRINKMANN K 1976 Circadian rhythm in the kinetics of acid denaturation of cell membranes of *Euglena gracilis*. Planta 129: 221–227
7. BRITZ SJ 1979 Chloroplast and nuclear migration. *In* W Haup, ME Feinleib, eds, Encyclopedia of Plant Physiology, Vol 7. Springer-Verlag, New York, pp 170–205
8. BRITZ SJ, WR BRIGGS 1976 Circadian rhythm of chloroplast orientation and photosynthetic capacity in *Ulva*. Plant Physiol 58: 22–27
9. BRODY S, SA MARTINS 1979 Circadian rhythms in *Neurospora crassa*: effects of unsaturated fatty acids. J Bacteriol 137: 912–915
10. BROWN DL, GB BOUCK 1973 Microtubule biogenesis and cell shape in *Ochromonas*. II. The role of nucleating sites in shape development. J Cell Biol 56: 360–378
11. CANDE WZ, MHM GOLDSMITH, PM RAY 1973 Polar auxin transport and auxin-induced elongation in the absence of cytoplasmic streaming. Planta 111: 279–296
12. CRAMER M, J MYERS 1952 Growth and photosynthetic characteristics of *Euglena gracilis*. Arch Mikrobiol 17: 384–402
13. EDMUNDS JR LN 1965 Studies on synchronously dividing cultures of *Euglena gracilis* Klebs (Strain Z). II. Patterns of biosynthesis during the cell cycle. Cell Comp Physiol 66: 159–182
14. EDMUNDS JR LN 1975 Temporal differentiation in *Euglena*: circadian phenomena in non-dividing populations and in synchronously dividing cells. *In* Les Cycles Cellulaires et Leur Blocage chez Plusieurs Protistes, Colloques Int CNRS No. 240. Centre National de la Recherche Scientifique, Paris, pp 53–67
15. EHRHARDT V, L RENSING 1976 Circadian rhythm of active amino acid transport in rat liver. J Interdiscipl Cycle Res 7: 287–290
16. FILNER P, NS YADAV 1979 Role of microtubules in intracellular movements. *In* W Haupt, ME Feinleib, eds, Encyclopedia of Plant Physiology New Series, Vol. 7. Springer-Verlag, New York, pp 95–113
17. GOTHAM IJ, HL FRISCH 1981 A simple model for cell volume and developmental compartments in nutrient limited cyclostat cultures of algae. J Theor Biol 92: 435–467
18. GUTTMAN HN, H ZIEGLER 1974 Clarification of structures related to function in *Euglena gracilis*. Cytobiologie 9: 10–22
19. HALABAN R 1975 Glucose transport-deficient mutant of *Neurospora crassa* with an unusual rhythmic growth pattern. J Bacteriol 121: 1056–1063
20. HOFMANN C, GB BOUCK 1976 Immunological and structural evidence for patterned intussusceptive surface growth in a unicellular organism: a postulated role for submembranous proteins and microtubules. J Cell Biol 69: 693–715
21. HUBER SC, GE EDWARDS 1975 Effect of DBMIB, DCMU, and antimycin A on cyclic and noncyclic electron flow in C_4 mesophyll chloroplasts. FEBS Lett 58:

211–214
22. KAUSS H 1979 Osmotic regulation in algae. *In* L Reinhold, ed, Progress in Phytochemistry, Vol 5. Pergamon Press, Oxford, pp 1–27
23. LIN S, DC LIN, JA SPUDICK, E KUN 1973 Inhibition of mitochondrial contraction by cytochalasin B. FEBS Lett 37: 241–243
24. LONERGAN TA 1981 A circadian rhythm in the rate of light-induced electron flow in three leguminous species. Plant Physiol 68: 1041–1046
25. LONERGAN TA, ML SARGENT 1978 Regulation of the photosynthesis rhythm in *Euglena gracilis*. I. Carbonic anhydrase and glyceraldehyde-3-phosphate dehydrogenase do not regulate the photosynthesis rhythm. Plant Physiol 61: 150–153
26. LONERGAN TA, ML SARGENT 1979 Regulation of the photosynthesis rhythm in *Euglena gracilis*. II. Involvement of electron flow through both photosystems. Plant Physiol 64: 99–103
27. MARCHANT HJ 1979 Microtubules cell wall deposition and the determination of plant cell shape. Nature 278: 167–168
28. MARCHANT HJ, JD PICKETT-HEAPS 1976 The effect of colchicine on colony formation in the algae *Hydrodictyon pediastrum* and *Sorastrum*. Planta 116: 291–300
29. MATTERN D, S BRODY 1979 Circadian rhythms in *Neurospora crassa*: effects of saturated fatty acids. J Bacteriol 139: 977–983
30. MCDANIEL M, C ROTH, J FINK, G FYFE, P LACY 1975 Effects of cytochalasins B and D on alloxan inhibition of insulin release. Biochem Biophys Res Commun 66: 1089–1096
31. ROHLF FJ, RR SOKAL 1969 *In* Statistical Tables. WH Freeman and Co, pp 129–135
32. SABNIS DD 1981 Lumicolchicine as a tool in the study of plant microtubules: some biological effects of sequential products formed during phototransformations of colchicine. J Exp Bot 32: 271–278
33. SCHONBOHM E 1973 Kontraktile Fibrillen als aktive Elemente bei der Mechanite der Chloroplastenverlagerung. Ber Dtsch Bot Ges 86: 407–422
34. SOKAL RR, FJ ROHLF 1969 *In* Biometry. WH Freeman and Co, pp 607–610
35. TANNER W, L DASCHEL, O KANDLER 1965 Effects of DCMU and antimycin A on photoassimilation of glucose in *Chlorella*. Plant Physiol 40: 1151–1156
36. WAGNER G, W HAUPT, A LAUX 1972 Reversible inhibition of chloroplast movement by cytochalasin B in the green alga *Mougeotia*. Science 176: 808–809
37. Yu KS, CA Mitchell, HA Robitaille 1979 Reevaluation of cyanide action in seed germination. Plant Physiol 63: 5–16